JOC Article

Self-Assembly with Degenerate Prototropy

Pranjal K. Baruah,[†] Rajesh Gonnade,[‡] Usha D. Phalgune,[§] and Gangadhar J. Sanjayan*,[†]

Division of Organic Synthesis, Central Material Characterization Division, and Central NMR Facility, National Chemical Laboratory, Dr. Homi Bhabha Road, Pune 411 008, India

sanjayan@ems.ncl.res.in

Received April 29, 2005

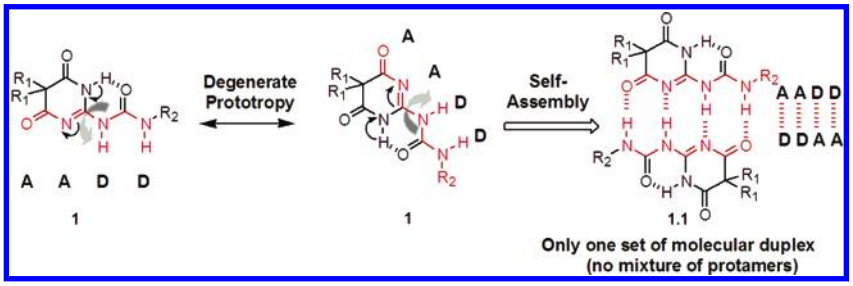

This work describes a rational approach for addressing the prototropy-related problems in heterocycle-based self-assembling systems by the use of *degenerate prototropy*. As a proof of principle, the utility of *degenerate prototropy* is demonstrated herein by developing heterocycle-based **AADD**-type self-assembling modules that exist as "single set of protameric pair (duplex)" in both solution and solid states. These self-assembling modules are quickly accessible in good yield by reacting 2-amino-5,5-disubstituted-1*H*-pyrimidine-4,6-diones, available in one step by the condensation of α,α-dialkyl malonates and free guanidine, with isocyanates. Evidence from NMR spectroscopy, ESI mass spectrometry, and single-crystal X-ray diffraction studies confirmed the formation of molecular duplexes. The effect of electronic repulsion in duplex formation is also investigated. Their ready synthetic accessibility, remarkably high propensity to crystal formation, and the novel property of *degenerate prototropy* would make these novel self-assembling molecules promising candidates for many proposed applications.

Introduction

Self-assembly, a process that creates structures through a statistical exploration of many possibilities, has emerged as a powerful tool for the construction of novel supramolecular architectures and nanomaterials with remarkable structural diversity and applications.[1−3] Owing to the directionality and specificity, hydrogen bonds are particularly useful for the programmed self-assembly of smaller molecular components to generate supramolecular ensembles with predefined structural features. To further enhance the strength, directionality, and specificity of hydrogen bonding interactions, there is currently intense research interest in designing self-assembling molecules having *arrays* of hydrogen bond donor (D) and acceptor (A) sites.[4,5] Among various such self-assembling modules reported thus far, heterocycle-based **AADD**-type self-complementary systems have ushered into promi-

[†] Division of Organic Synthesis.
[‡] Central Material Characterization Division.
[§] Central NMR Facility.

(1) (a) Lehn, J.-M. *Supramolecular Chemistry: Concepts and Perspectives*; VCH: Weinheim, Germany, 1995. (b) Steed, J. W.; Atwood, J. L. *Supramolecular Chemistry*; Wiley: New York, 2000. (c) Whitesides, G. M.; Grzybowski, B. *Science* **2002**, *295*, 2418−2421. (d) Bushey, M. L.; Nguyen, T.-Q.; Zhang, W.; Horoszewski, D.; Nuckolls, C. *Angew. Chem., Int. Ed.* **2004**, *43*, 5446−5453. (e) Conn, M. M.; Rebek, J., Jr. *Chem. Rev.* **1997**, *97*, 1647−1668. (f) Lindsey, J. S. *New J. Chem.* **1991**, *15*, 153−180. (g) Fredericks, J. R.; Hamilton, A. D. In *Comprehensive Supramolecular Chemistry*; Sauvage, J.-P., Hosseini, M. W., Eds.; Pergamon Press: Oxford, 1996; Vol. IX, Chapter 16. (h) Hill, D. J.; Mio, M. J.; Prince, R. B.; Hughes, T. S.; Moore, J. S. *Chem. Rev.* **2001**, *101*, 3893−4011. (i) Sessler, J. L.; Jayawickramarajah, J. *Chem. Commun*. **2005**, 1939−1949.

(2) (a) Zhang, W.; Liao, S. S.; Cui, F. Z. *Chem. Mater*. **2003**, *15*, 3221−3226. (b) Erma, S.; Hauck, T.; El-Khouly, M. E.; Padmawar, P. A.; Canteenwala, T.; Pritzker, K.; Ito, O.; Chiang, L. Y. *Langmuir* **2005**, *21*, 3267−3272. (c) Hu, W.; Nakashima, H.; Furukawa, K.; Kashimura, Y.; Ajito, K.; Liu, Y.; Zhu, D.; Torimitsu, K. *J. Am. Chem. Soc*. **2005**, *127*, 2804−2805. (d) Tsonchev, S.; Schatz, G. C.; Ratner, M. A. *J. Phys. Chem. B* **2004**, *108*, 8817−8822.

(3) (a) Whitesides, G. M.; Mathias, J. P.; Seto, C. T. *Science* **1991**, *254*, 1312−1319. (b) Hummer, G.; Garde, S.; Garcia, A. E.; Paulaitis, M. E.; Pratt, L. R. *J. Phys. Chem. B* **1998**, *102*, 10469−10482. (c) Bowden, N.; Choi, I. S.; Grzybowski, B. A.; Whitesides, G. M. *J. Am. Chem. Soc*. **1999**, *121*, 5373−5391. (d) Bowden, N.; Terfort, A.; Carbeck, J.; Whitesides, G. M. *Science* **1997**, *276*, 233−235. (e) Wu, H.; Bowden, N.; Whitesides, G. M. *Appl. Phys. Lett*. **1999**, *75*, 3222−3224. (f) Choi, I. S.; Bowden, N.; Whitesides, G. M. *Angew. Chem., Int. Ed.* **1999**, *38*, 3078−3081.

10.1021/jo0508705 CCC: $30.25
Published on Web 07/09/2005

nence primarily due to their relatively high dimerization constants coupled with ready synthetic accessibility. Of particular interest are the dimers of **AADD**-type self-complementary arrays, developed independently by Meijer's[6] and Zimmerman's[7] groups, that are stable in nonpolar solvents in a wide concentration range, making them excellent building blocks for supramolecular architectures and polymers.[8] However, the generality of self-assembling systems based on rigid heterocycles is sometimes complicated by prototropy[9] that is often associated with heterocycles. Furthermore, the supramolecular polymers derived from such prototropy-prone heterocycle-based self-assembling modules can exist in multiple prototropic forms, rendering their structural studies tricky.[10]

Here we introduce for the first time the use of degenerate prototropy as a means to develop heterocycle-based self-assembling systems free of prototropy-related problems. As a proof of principle, the utility of degenerate prototropy is demonstrated herein by developing heterocycle-based **AADD**-type self-assembling modules that exist as a single set of protameric pair (duplex) in both solution and solid states. The strategy disclosed herein has the potential for significantly augmenting the "tool box" of the modern day supramolecular chemist, as well as providing a novel approach to the field of rational design using the concept of degenerate prototropy.

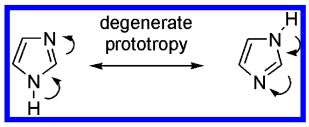

FIGURE 1. Degenerate prototropy in imidazole.

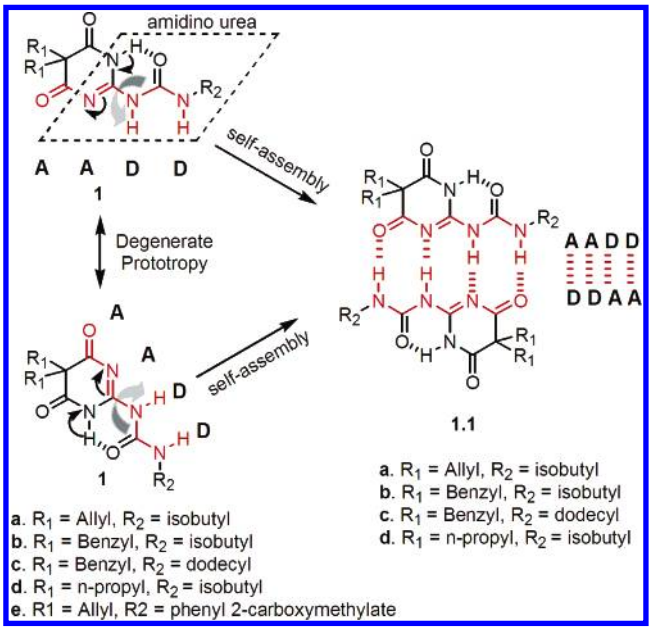

FIGURE 2. Degenerate prototropy in **1**. Block arrows indicate rotation (180°) of urea moiety about the bond connecting the heterocycle.

Design Principles. Degenerate prototropy, also known as degenerate tautomerism, is a phenomenon by which annular prototropic shift regenerates the same structure due to the chemical equivalence of the protamers.[11] One of the simplest systems that exhibit degenerate prototropy is imidazole wherein both the protamers, formed by 1,3-annular prototropic shift, are rendered equivalent by prototropic degeneracy (Figure 1).

Though a number of systems have been shown to exhibit this fascinating phenomenon,[12] its utility as a nifty concept in the rational design of novel systems largely remains unexplored. To tackle the multiple protamer formations in heterocycle-based **AADD**-type self-assembling systems, we designed the urea construct **1** (Figure 2).

The design principles were based on the observation that 1,3 annular prototropic shift in heterocycles such as imidazole results in prototropic degeneracy due to the chemical equivalence of the protamers. It was anticipated that acylation of the amidino urea moiety with a symmetrical bis-acyl unit, as in **1**, should provide the molecule sufficient room for degenerate prototropy. In the urea construct **1**, the amidino urea moiety is tethered to an α,α-disubstituted malonyl unit such that annular 1,3

(4) For excellent reviews, see: (a) Brunsveld, L.; Folmer, B. J. B.; Meijer, E. W.; Sijbesma, R. P. *Chem. Rev.* **2001**, *101,* 4071−4097. (b) Sijbesma, R. P.; Meijer, E. W. *Chem. Commun*. **2003**, 5−16. (c) Zimmerman, S. C.; Corbin, P. S. *Struct. Bonding (Berlin)* **2000**, *96*, 63−94. (d) Schmuck, C.; Wienand, W. *Angew. Chem., Int. Ed*. **2001**, *40*, 4363−4369.

(5) (a) Yang, X.; Gong, B. *Angew. Chem., Int. Ed*. **2005**, *44*, 1352−1356. (b) Yang, X.; Hua, F.; Yamato, K.; Ruckenstein, E.; Gong, B.; Kim, W.; Ryu, C. Y. *Angew. Chem., Int. Ed*. **2004**, *43*, 6471−6474. (c) Schmuck, C.; Wienand, W. *J. Am. Chem. Soc*. **2003**, *125*, 452−459. (d) Schmuck, C. *Chem.−Eur. J*. **2000**, *6*, 709−718. (e) Schmuck, C.; Geiger, L. *J. Am. Chem. Soc.* **2004**, *126*, 8898−8899. (f) Zeng, H.; Yang, X.; Brown, A. L.; Martinovic, S.; Smith, R. D.; Gong, B. *Chem. Commun.* **2003**, 1556−1557. (g) Zhao, X.; Wang, X.-Z.; Jiang, X.-K.; Chen, Y.-Q.; Li, Z. -T.; Chen, G.-J. *J. Am. Chem. Soc.* **2003**, *125*, 15128−15139. (h) Davis, A. P.; Draper, S. M.; Dunnea, G.; Ashtonb, P. *Chem. Commun.* **1999**, 2265−2266. (i) Lüning, U.; Kühl, C.; Uphoff, A. *Eur. J. Org. Chem.* **2002**, 4063−4070.

(6) (a) Beijer, F. H.; Sijbesma, R. P.; Kooijman, H.; Spek, A. L.; Meijer, E. W. *J. Am. Chem. Soc.* **1998**, *120*, 6761−6769. (b) Cate, A. T.; Kooijman, H.; Spek, A. L.; Sijbesma, R. P.; Meijer, E. W. *J. Am. Chem. Soc.* **2004**, *126*, 3801−3808. (c) Ligthart, G. B. W. L.; Ohkawa, H.; Sijbesma, R. P.; Meijer, E. W. *J. Am. Chem. Soc.* **2005**, *127*, 810−811 and references therein.

(7) (a) Corbin, P. S.; Zimmerman, S. C. *J. Am. Chem. Soc.* **1998**, *120*, 9710−9711. (b) Corbin, P. S.; Lawless, L. J.; Li, Z.; Ma, Y.; Witmer, M. J.; Zimmerman, S. C. *Proc. Natl. Acad. Sci. U.S.A.* **2002**, *99*, 5099−5104.

(8) Meijer's ureidopyrimidinone self-assembling modules have been extensively used for supramolecular polymer synthesis. See: (a) Sijbesma, R. P.; Beijer, F. H.; Brunsveld, L.; Folmer, B. J. B.; Hirschberg, J. H. K. K.; Lange, R. F. M.; Lowe, J. K. L.; Meijer, E. W. *Science* **1997**, *278*, 1601−1604. (b) Hirschberg, J. H. K. K.; Beijer, F. H.; van Aert, H. A.; Magusin, P. C. M. M.; Sijbesma, R. P.; Meijer, E. W. *Macromolecules* **1999**, *32*, 2696−2705. (c) Folmer, B. J. B.; Sijbesma, R. P.; Versteegen, R. M.; van der Rijt, J. A. J.; Meijer, E. W. *Adv. Mater.* **2000**, *12*, 874−878.

(9) Due to prototropy, Zimmerman's pyrido-pyrimidinone-based self-assembling system exists in as many as four protamers (see ref 7a), and Meijer's ureidopyrimidinone has been shown to display mainly two types of protamer formation, depending upon the substitution pattern on the heterocyclic ring (see ref 6a).

(10) The tautomeric rearrangement of supramolecular polymers having ureidopyrimidinone self-assembling modules had been investigated by ^{1}H DQ NMR spectroscopy under fast MAS conditions. See: Schnell, I.; Langer, B.; Sontjens, S. H. M.; Sijbesma, R. P.; van Genderen, M. H. P.; Spiess, H. W. *Phys. Chem. Chem. Phys*. **2002**, *4*, 3750−3758.

(11) Elguero, J.; Marzin, C.; Katritzky, A. R.; Linda, P. *The Tautomerism of Heterocycles: Advances in Heterocyclic Chemistry*; Academic Press: New York, 1976.

(12) (a) Komber, H.; Limbach, H. H.; Boehme, F.; Kunert, C. *J. Am. Chem. Soc.* **2002**, *124*, 11955−11963. (b) Maki, J.; Klika, K. D.; Sjoholm, R.; Kronberg, L. *J. Chem. Soc., Perkin Trans. 1* **2001**, 1216−1219. (c) Thoburn, J. D.; Luettke, W.; Benedict, C.; Limbach, H. H. *J. Am. Chem. Soc*. **1996**, *118*, 12459−12460. (d) Helaja, J.; Montforts, F. P.; Kilpelaeinen, I.; Hynninen, P. H. *J. Org. Chem*. **1999**, *64*, 432−437.

SCHEME 1. Synthesis of 1a−e[a]

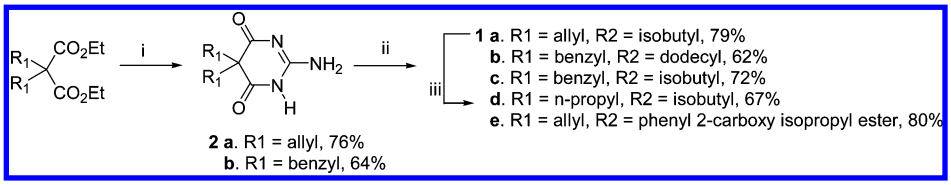

[a] Reagents and conditions: (i) NaOEt, EtOH, guanidine HCl, reflux, 4h. (ii) R_2NCO, pyridine, 90−100 °C, 2h. (iii) H_2/Pd−C (10%).

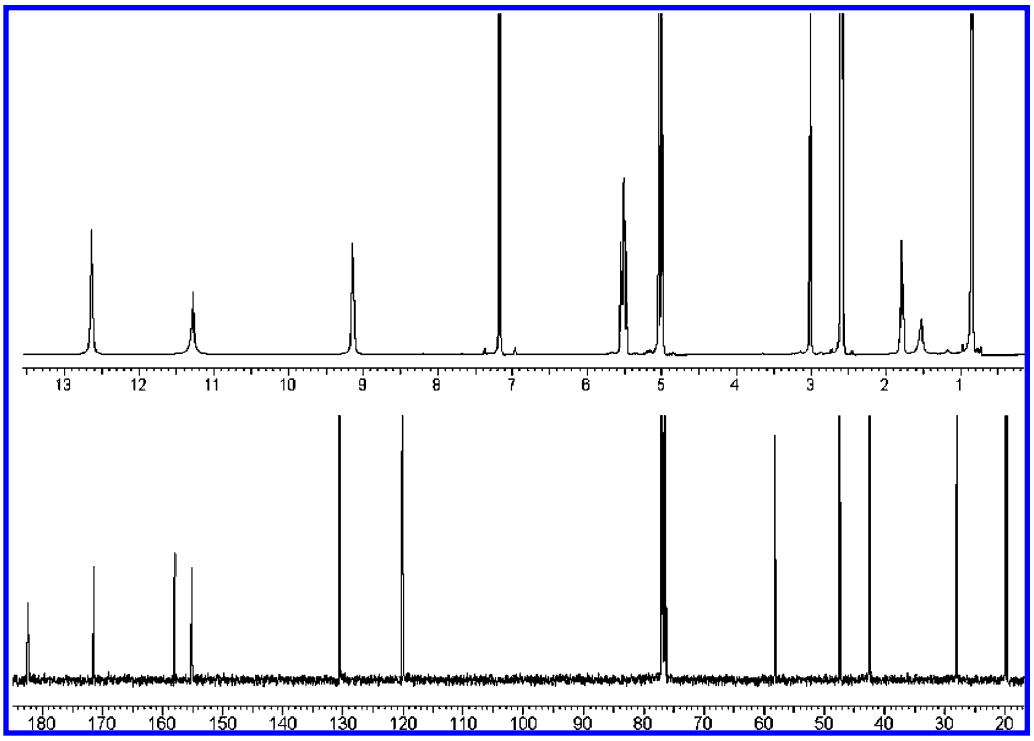

FIGURE 3. ^{1}H [top (500 MHz)] and ^{13}C [bottom (125 MHz)] NMR spectra of **1a** in $CDCl_3$ showing single set of well-resolved signals.

prototropic shift, accompanied by the 180° rotation of the urea moiety[13] about the bond connecting the heterocyclic ring, would result in prototropic degeneracy, since the protamers would be, in all respects, equivalent. Thus, the dimerization of **1** can be expected to lead to only a single set of hydrogen-bonded duplex. Structural studies, vide infra, indeed showed that **1** forms only a single set of molecular duplex **1.1** in both solution and solid states.

Results and Discussion

Urea construct **1** is quickly accessible in good yield by reacting 2-amino-5,5-disubstituted-1*H*-pyrimidine-4,6-diones, available in one step by the condensation of α,α-dialkyl malonates and free guanidine,[14] with isocyanates in pyridine (Scheme 1).

Contrary to its precursors, **1** was highly soluble in nonpolar organic solvents including petroleum ether (≫100 mM in petroleum ether) at ambient temperature. This observation suggested that the polar hydrogen-bonding groups of **1** were strongly protected by dimerization, preventing the formation of polymeric aggregates.[15] ^{1}H and ^{13}C NMR (500 and 125 MHz, respectively) spectra of **1a** in $CDCl_3$ show a single set of well-resolved signals[16] (Figure 3).

The significant downfield NH chemical shifts were indicative of strong hydrogen-bonding interactions in solution. Both urea NH signals of **1a**, appearing at 9.24 and 11.38 ppm, showed concentration-dependent changes in their chemical shifts, supporting their role in forming intermolecular hydrogen bonding. The NH group (12.74 ppm) involved in the formation of the intramolecular S(6) ring[17] that pre-fixes the linear **AADD** hydrogen-bonding array showed an insignificant concentration-dependent shift. ^{1}H NMR binding studies,[18] in the concentration range of 100−0.5 mM range, gave the dimerization constant (K_{dim}) 1.2×10^4 M^{-1} for **1a** in $CDCl_3$.[19]

(13) The amide bond prefers trans geometry. See: Katrizky, A. R.; Ghiviriga, I. *J. Chem. Soc., Perkin Trans. 2* **1995**, 1651−1653.

(14) Lehn, J.-M.; Mascal, M.; DeCian, A.; Fischer, J. *J. Chem. Soc., Perkin Trans. 2* **1992**, 461−467.

(15) (a) Similar observation has been reported by Whitesides's group for the solubility of hydrogen-bonded aggregates: Mathias, J. P.; Simanek, E. E.; Whitesides, G. M. *J. Am. Chem. Soc.* **1994**, *116*, 4326−4340. (b) For the use of hydrogen bonds to control molecular aggregation, see also: Simard, M.; Su, D.; Wuest, J. D. *J. Am. Chem. Soc.* **1991**, *113*, 4696−4698.

(16) Separate sets of NMR signals become evident if more than one protamer exists in solution; see refs 6a and 7a.

(17) Etter, M. C. *Acc. Chem. Res.* **1990**, *23*, 120−126.

(18) Wilcox, C. S. In *Frontiers in Supramolecular Chemistry and Photochemistry*; Schneider, H. J., Durr, H., Eds.; VCH: Weinheim, Germany, 1990; pp 123−144.

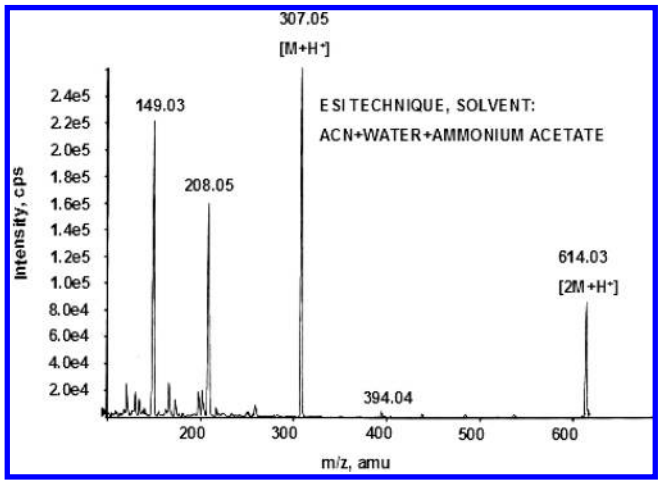

FIGURE 4. ESI mass spectrum of **1a**.

ESI mass spectrometry is an effective tool in investigating the formation of hydrogen-bonded molecular self-assemblies. The formation of discrete dimers **1.1** was further confirmed by ESI mass spectrometry. In addition to the molecular ion peaks (MH^+) ascribable due to the monomers **1**, the ESI spectrum (Figure 4) showed sizable peaks corresponding to the dimers **1.1** (M_2H^+).

An interesting property associated with the self-assembling systems reported herein is their remarkably high propensity to easily crystallize into large crystals under ambient conditions, presumably as a consequence of the intrinsic nature of rigid α,α-dialkylated systems to efficiently pack into crystalline lattices.[20] It is noteworthy that hydrogen-bonded self-assembling systems usually show a poor tendency to crystallize under ordinary conditions, presumably due to their inefficient packing in crystalline lattices.[21] This has prompted researchers to utilize drastic conditions to crystallize self-assembling organic systems, using high pressure and temperature,[22] a condition routinely used for crystallizing quartz, zeolites, and inorganic open-frame structures.[23] The solid-state structures of **1a**−**c** were determined by single-crystal X-ray diffraction[24] (Figure 5). Comparison of the X-ray structures of **1a**−**c** reveals the following facts. All three compounds, irrespective of the nature of substituents, form centrosymmetric dimers **1.1** in the solid state, maintaining similar hydrogen-bonding codes.[25] The dimers are held together by four C(4)-type[17] intermolecular hydrogen bonds between self-complementary **AADD**-type linear hydrogen-bonding arrays.

The urea functionality is in a *trans*−*trans* geometry, as expected, and an intramolecular S(6)-type[17] hydrogen bond bridges the pyrimidine N−H to the urea carbonyl group that preorganizes the **AADD** array of hydrogen bonding sites. In all the cases, the **AADD** array deviates slightly from linearity, the outer N−H···O hydrogen bonds being somewhat shorter than the inner N−H···N hydrogen bonds.

Interestingly, the dimer **1.1a** forms self-assembled infinite chains of helical nature (Figure 6) through a relatively weaker bifurcated intermolecular hydrogen bonding involving the pyrimidine ring N−H and the remaining carbonyl group of another molecule forming an eight-membered ring hydrogen-bonded network, although similar arrangement is not observed in **1.1b** and **1.1c**. The eight-membered ring hydrogen-bonded network, formed by the self-assembly of the duplexes, is characterized by the graph set $R^2_2(8)$.[17] The bifurcated hydrogen bonds in the extended self-assembled network of **1.1a** are relatively weaker because the D−H···A distances are longer [d(H···O) = 2.464 and 2.526 Å].

Although a highly symmetrical pattern of hydrogen bonding is maintained in **1b**, a similar trend is absent in **1a** and **1c**. Notably, in **1.1c**, the hydrogen-bonding arrays are considerably forced out of plane presumably due to the steric clash between benzyl and isobutyl substituents, though such an interaction does not prevent dimer formation.

Effect of Electronic Hindrance in Duplex Formation. Substituents are known to play a crucial role in dictating the mode of association of self-assembling systems, either through steric hindrance[27] or through hyperconjugation effects.[6a] Whitesides et al. have cleverly made use of steric hindrance as a major driving force in specifically obtaining cyclic rosette, tape, or crinkled tape self-assembled structures using the melamine-cyanuric acid self-assembling motifs.[27] In an effort to evaluate the influence of electronic hindrance in duplex formation, we designed and synthesized the self-complementary motif **1e**, having an *o*-carboxymethyl phenyl substituent tethered to the urea moiety. **1e** was highly soluble in nonpolar organic solvents, suggesting that the protons were solvent-shielded. Observation of 2M+ peak in the ESI mass spectrum also strongly suggested the dimer formation (see Supporting Information).

In stark contrast to such findings, surprisingly, the duplex formation through quadruple intermolecular hydrogen bonding could not be observed in the solid state as unambiguously confirmed by single-crystal X-ray studies. Instead of dimerization, **1e** formed an extended sheetlike structure through intermolecular hydrogen bonding (Figure 7). Analysis of the single-crystal structure of **1e** revealed the presence of two intramolecular

(19) This value is relatively low when compared to the dimerization constant (K_{dim}) of Meijer's **AADD**-type ureidopyrimidinones containing a heterocyclic aromatic unit that is in *keto*−*enol* tautomeric equilibrium (see ref 6a). The relatively low K_{dim} of the present system is presumably due to the absence of π-electron density in the heterocyclic ring that could have positively contributed to the duplex stability as in ureidopyrimidinones. For a related example, see: Lafitte, V. G. H.; Aliev, A. E.; Hailes, H. C.; Bala, K.; Golding, P. *J. Org. Chem.* **2005**, *70*, 2701−2707.

(20) Karle, I. L. *Acta Crystallogr., Sect. B* **1992**, *48*, 341−356.

(21) *Comprehensive Supramolecular Chemistry*; Atwood, J. L., Davies, J. E. D., MacNicol, D. D., Vogtle, F., Eds.; Pergamon Press: Oxford, 1996; Vol. 9, pp 671−700.

(22) Ranganathan, A.; Pedireddi, V. R.; Rao, C. N. R. *J. Am. Chem. Soc*. **1999**, *121*, 1752−1753.

(23) Rao, C. N. R. *Chemical Approaches to the Synthesis of Inorganic Materials*; Wiley: New York, 1993.

(24) The crystal structures of **1a**−**c**,**e** were solved by direct method using SHELXS-97, and the refinement was performed by full matrix least squares of F^2 using SHELXL-97 (Sheldrick, G. M. *SHELX-97*, program for crystal structure solution and refinement; University of Göttingen: Göttingen, Germany, 1997). Hydrogen atoms were included in the refinement as per the riding model. CIF files are available in Supporting Information.

(25) Substituents can influence the mode of hydrogen bonding (hydrogen-bonding codes) in dimer formation; see ref 6a.

(26) Delano, W. L. *The PyMOL Molecular Graphics System*; http://www.pymol.org, 2004.

(27) Whitesides, G. M.; Simanek, E. E.; Mathias, J. P.; Seto, C. T.; Chin, D. N.; Mammen, M.; Gordon, D. M. *Acc. Chem. Res.* **1995**, *28*, 37−44.

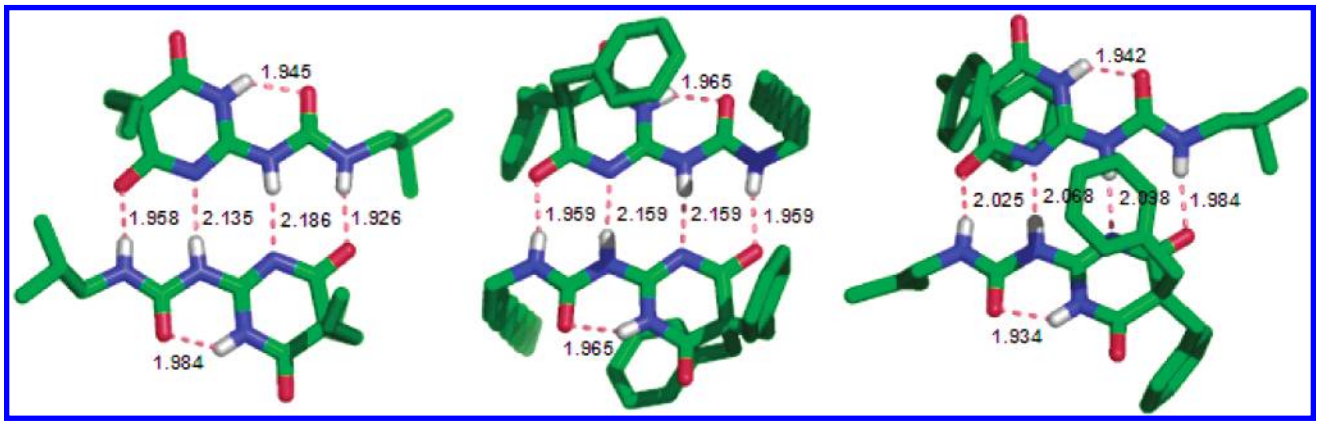

FIGURE 5. Single-crystal X-ray structures of dimers **1.1a** (left), **1.1b** (middle), and **1.1c** (right). Hydrogen bonding is highlighted in dashes (salmon colored), above which hydrogen bond distances (NH···N and NH···O) are displayed in Å. All hydrogens, other than those at the hydrogen-bonding sites, have been deleted for clarity. This figure was made using PyMOL.[26]

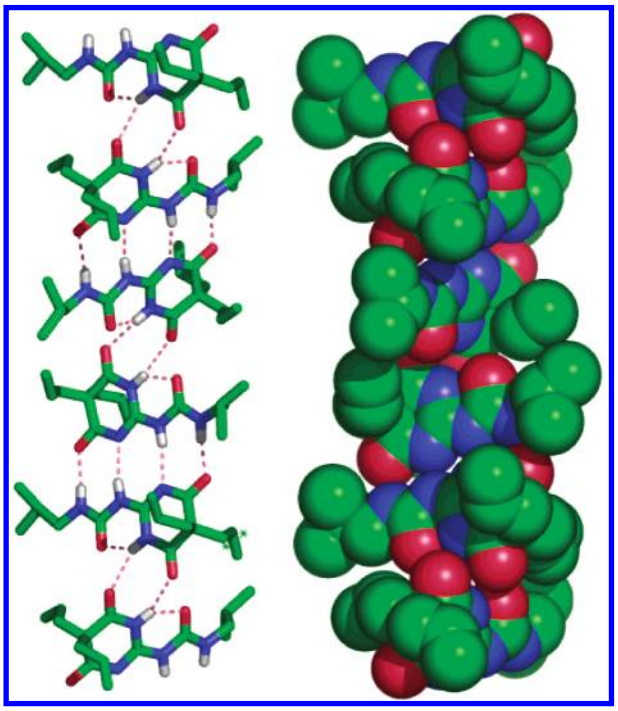

FIGURE 6. Further self-assembly of **1.1a**, both capped stick (left) and sphere (right) representations, showing infinite chains of helical nature. All hydrogens have been deleted for clarity in the sphere representation. This figure was made using PyMOL.[26]

hydrogen bonding within the molecule, as expected. Interestingly, unlike in **1a**−**c**, the **AADD**-type hydrogen-bonding linear array is nonexistent in **1e**. The nonformation of duplex **1.1e** is presumably due to the unfavorable electronic repulsion that would have resulted by the close proximity of the anthranilic acid carbonyls and the heterocyclic carbonyls in the duplex **1.1e**.

Summary

In summary, this article describes a rational approach for addressing the prototropy-related problems in heterocycle-based self-assembling systems by the use of degenerate prototropy. As a proof of principle, we demonstrated herein the utility of degenerate prototropy in designing heterocycle-based **AADD**-type self-assembling

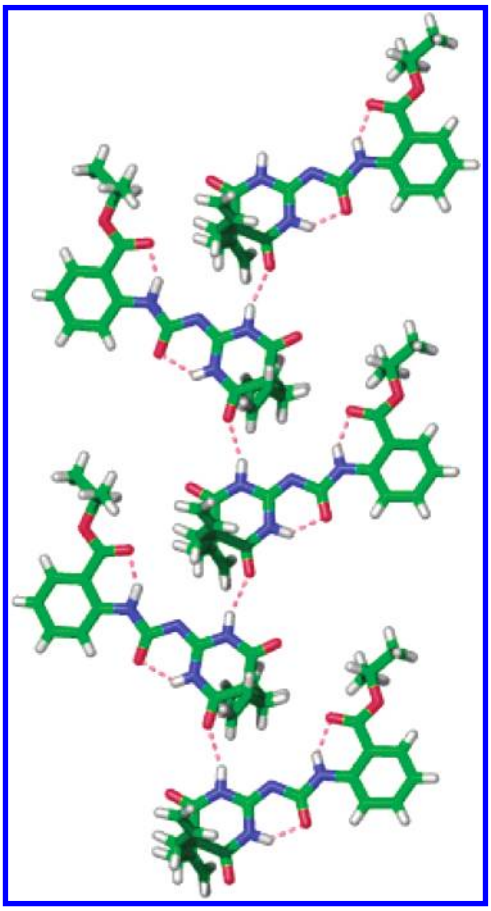

FIGURE 7. Single-crystal X-ray structure of **1e** showing self-assembly, through intermolecular hydrogen bonding, forming one-dimensional sheetlike network. This figure was made using PyMOL.[26]

constructs free of multiple protamers. Our unique design strategy has allowed for an added dimension in the self-assembled H-bonded molecular duplexes reported herein, drawing a stark distinction between itself and previously known systems having similar hydrogen bonding codes.[6,7] Their ready synthetic accessibility coupled with the novel property of degenerate prototropy and the great ease of crystal formation would make these novel self-assembling molecules promising candidates for many proposed ap-

plications. We are currently probing their utility for the construction of supramolecular polymers and will report the results in due course.

Experimental Section

Single-Crystal X-ray Crystallographic Studies. The X-ray data of **1a**−**c**,**e** were collected on a SMART APEX CCD diffractometer with ω and φ scan mode, $\lambda_{MoK\alpha} = 0.71073$ Å at $T = 133(2)$ K. All the data were corrected for Lorentzian, polarization, and absorption effects using the SAINT and SADABS programs. The crystal structures of **1a**−**c**,**e** were solved by direct method using SHELXS-97, and the refinement was performed by full matrix least squares of F^2 using SHELXL-97[24]. Hydrogen atoms were included in the refinement as per the riding model.

Crystal data for **1a** ($C_{15}H_{22}N_4O_3$): $M = 306.37$, crystal dimensions $0.75 \times 0.65 \times 0.25$ mm^3, triclinic, space group $P\bar{1}$, $a = 13.5798(18)$, $b = 14.1602(19)$, $c = 17.503(2)$ Å, $\alpha = 91.381(2)°$, $\beta = 94.924(2)°$, $\gamma = 98.849(2)°$, $V = 3311.0(8)$ Å^3, $Z = 8$; $\rho_{calcd} = 1.229$ gcm^{-3}, μ(Mo Kα) = 0.087 mm^{-1}, $F(000) = 1312$, $2\theta_{max} = 50.00°$, 31 720 reflections collected, 11 607 unique, 9602 observed ($I > 2\sigma(I)$) reflections, 827 refined parameters, R value 0.0440, $wR2 = 0.1146$ (all data $R = 0.0537$, $wR2 = 0.1216$), $S = 1.051$, minimum and maximum transmission 0.9373 and 0.9785, respectively, maximum and minimum residual electron densities +0.427 and −0.306 e Å^{-3}.

Crystal data for **1b** ($C_{31}H_{42}N_4O_3$): $M = 518.69$, crystal dimensions $0.94 \times 0.09 \times 0.03$ mm^3, triclinic, space group $P\bar{1}$, $a = 6.467(4)$, $b = 13.910(8)$, $c = 16.488(10)$ Å, $\alpha = 90.717(11)°$, $\beta = 91.918(11)°$, $\gamma = 95.011(11)°$, $V = 1476.6(15)$ Å^3, $Z = 2$; $\rho_{calcd} = 1.167$ gcm^{-3}, μ(Mo Kα) = 0.076 mm^{-1}, $F(000) = 560$, $2\theta_{max} = 50.00°$, 10 631 reflections collected, 5176 unique, 2703 observed ($I > 2\sigma(I)$) reflections, 344 refined parameters, R value 0.0553, $wR2 = 0.0992$ (all data $R = 0.1255$, $wR2 = 0.1202$), $S = 0.939$, minimum and maximum transmission 0.9323 and 0.9977, respectively, maximum and minimum residual electron densities +0.152 and −0.154 e Å^{-3}.

Crystal data for **1c** ($C_{23}H_{26}N_4O_3$): $M = 406.48$, crystal dimensions $0.70 \times 0.68 \times 0.13$ mm^3, monoclinic, space group $P2_1/n$, $a = 23.675(3)$, $b = 18.479(3)$, $c = 30.427(4)$ Å, $\beta = 100.690(3)°$; $V = 13\,081(3)$ Å^3; $Z = 24$; $\rho_{calcd} = 1.238$ gcm^{-3}, μ(Mo Kα) = 0.084 mm^{-1}, $F(000) = 5184$, $2\theta_{max} = 50.00°$, 64 574 reflections collected, 22 995 unique, 14 350 observed ($I > 2\sigma(I)$) reflections, 1685 refined parameters, R value 0.0647, $wR2 = 0.1495$ (all data $R = 0.1109$, $wR2 = 0.1693$), $S = 1.014$, minimum and maximum transmission 0.9437 and 0.9892, respectively, maximum and minimum residual electron densities +0.725 and −0.420 e Å^{-3}.

Crystal data for **1e** ($C_{21}H_{24}N_4O_5$): $M = 412.44$, crystal dimensions $0.67 \times 0.41 \times 0.29$ mm^3, triclinic, space group $P\bar{1}$, $a = 12.065(9)$, $b = 13.786(10)$, $c = 14.428(10)$ Å, $\alpha = 98.58(3)°$, $\beta = 108.43(2)°$, $\gamma = 100.28(2)°$, $V = 2185(3)$ Å^3, $Z = 4$; $\rho_{calcd} = 1.254$ gcm^{-3}, μ(Mo Kα) = 0.091 mm^{-1}, $F(000) = 872$, $2\theta_{max} = 50.00°$, 10 384 reflections collected, 6921 unique, 4800 observed ($I > 2\sigma(I)$) reflections, 569 refined parameters, R value 0.0762, $wR2 = 0.2161$ (all data $R = 0.1031$, $wR2 = 0.2461$), $S = 1.044$, minimum and maximum transmission 0.9416 and 0.9741, respectively, maximum and minimum residual electron densities +0.553 and −0.298 e Å^{-3}.

Experimental Procedures. 5,5-Diallyl-2-amino-1*H*-pyrimidine-4,6-dione[14] 2a. Sodium metal (4.66 g, 202.6 mmol, 3.04 equiv) was dissolved carefully in absolute ethanol (56 mL). To the above solution was added α,α-diallyl-malonic acid diethyl ester (16 g, 66.6 mmol, 1 equiv) followed by the addition of guanidine hydrochloride (10.83 g, 113.3 mmol, 1.7 equiv). The reaction mixture was refluxed for 4 h, cooled, and filtered through Celite. The filtrate was acidified with aqueous acetic acid, and the precipitated amino pyrimidine was filtered, washed with water, and dried. The product was purified by crystallization from aqueous DMSO (10.5 g, 76%). mp > 260 °C; IR (Nujol) ν (cm^{-1}): 3238, 3193, 2947, 2923, 2854, 1730, 1695, 1649, 1485, 1390; ^{1}H NMR (Na salt) (300 MHz, D_2O): δ 5.49−5.35 (m, 2H), 4.91 (t, 4H, $J = 8.7$ Hz), 2.43 (d, 4H, $J = 6.4$ Hz); ^{13}C NMR (Na salt) (75 MHz, D_2O): δ 200.8, 182.9, 145.8, 131.3, 68.1, 55.3; ESI Mass: 208.05 (M + 1); Anal. Calcd for $C_{10}H_{13}N_3O_2$: C, 57.96; H, 6.32; N, 20.28. Found: C, 57.67; H, 6.53; N, 20.11.

2-Amino-5,5-dibenzyl-1*H*-pyrimidine-4,6-dione 2b. Following the similar procedure for the synthesis of **2a** and using α,α-dibenzyl-malonic acid diethyl ester (15.02 g, 44.1 mmol), **2b** was synthesized which was purified by crystallization from aqueous DMSO (8.7 g, 64%). mp > 260 °C; IR (Nujol) ν (cm^{-1}): 3240, 3197, 2923, 2854, 1689, 1454, 1384; ^{1}H NMR (500 MHz, DMSO-d_6): δ 10.44 (s, 1H), 7.21−7.02 (m, 12H), 3.18 (s, 4H); ^{13}C NMR (125 MHz, DMSO-d_6): δ 177.1, 157.2, 136.4, 129.5, 128.2, 126.9, 59.0, 44.5; ESI Mass: 308.04 (M + 1); Anal. Calcd for $C_{18}H_{17}N_3O_2$: C, 70.34; H, 5.58; N, 13.67. Found: C, 69.97; H, 5.74; N, 13.69.

1-(5,5-Diallyl-4,6-dioxo-1,4,5,6-tetrahydro-pyrimidin-2-yl)-3-isobutyl-urea 1a. To a stirred solution of dry dichloromethane (10 mL) at 0 °C containing triphosgene (2.71 g, 9.1 mmol, 0.63 equiv) was added a mixture of isobutylamine (2.61 mL, 26.1 mmol, 1.8 equiv) and *N*-ethyldiisopropylamine (9.81 mL, 57.3 mmol, 3.96 equiv) dissolved in dry DCM (5 mL) dropwise. After being stirred for 10 min at 0 °C, dry pyridine (40 mL) was added to the above reaction mixture, followed by the addition of 5,5-diallyl-2-amino-1*H*-pyrimidine-4,6-dione (3.0 g, 14.5 mmol, 1 equiv). The reaction mixture was heated on an oil bath held at 90−100 °C for 2 h. After cooling, the reaction mixture was filtered off, and the solvents were removed under vacuum. The residue was dissolved in ethyl acetate and was washed with water and brine. The organic layer was dried with anhydrous sodium sulfate and concentrated under reduced pressure. The crude product was purified by column chromatography (5% ethyl acetate/petroleum ether) on silica gel to give 3.52 g (79%) of **1a** as colorless crystalline solid which could be further easily crystallized from petroleum ether (60−80 °C) to give large crystals. mp 121 °C; IR ($CHCl_3$) ν (cm^{-1}): 3232, 3076, 3026, 2964, 1706, 1614, 1571, 1529, 1245; ^{1}H NMR (500 MHz, $CDCl_3$): δ 12.74 (s, 1H), 11.38 (s, 1H), 9.24 (s, 1H), 5.66−5.58 (m, 2H), 5.11 (t, 4H, $J = 13.6$ Hz), 3.11 (t, 2H, $J = 6.2$ Hz), 2.70 (d, 4H, $J = 7.4$ Hz), 1.8 (sept, 1H, $J = 6.7$ Hz), 0.95 (d, 6H, $J = 6.6$ Hz); ^{13}C NMR (125 MHz, $CDCl_3$): δ 182.7, 171.8, 158.3, 155.5, 131.0, 120.4, 58.5, 47.8, 42.8, 28.3, 20.1; ESI Mass: 307.05 (M + 1), 614.03 (2M + 1); Anal. Calcd for $C_{15}H_{22}N_4O_3$: C, 58.81; H, 7.24; N, 18.29. Found: C, 58.53; H, 7.45; N, 18.18.

1-(5,5-Dibenzyl-4,6-dioxo-1,4,5,6-tetrahydro-pyrimidin-2-yl)-3-dodecyl-urea 1b. Following the similar procedure for the synthesis of **1a** and using 2-amino-5,5-dibenzyl 1*H*-pyrimidine-4,6-dione (1.1 g, 3.6 mmol), **1b** was synthesized (1.19 g, 62%), which was easily crystallized from petroleum ether into large crystals. mp 72−73 °C; IR ($CHCl_3$) ν (cm^{-1}): 3230, 3020, 2927, 2854, 1703, 1612, 1569, 1529, 1245, 1215; ^{1}H NMR (500 MHz, $CDCl_3$): δ 12.28 (s, 1H), 10.52 (s, 1H), 8.94 (s, 1H), 7.23−7.08 (m, 10H), 3.36 (q, 4H, $J = 13$, 11.5 Hz), 3.23 (q, 2H, $J = 6.9$, 5.4 Hz), 1.61 (q, 2H, $J = 6.9$ Hz), 1.38−1.25 (b, 18H), 0.88 (t, 3H, $J = 6.9$ Hz); ^{13}C NMR (125 MHz, $CDCl_3$): δ 182.0, 171.8, 157.2, 155.2, 135.1, 129.6, 128.4, 127.4, 62.1, 45.1, 40.3, 31.9, 29.6, 29.4, 29.3, 29.2, 27.0, 22.6, 14.0; ESI Mass: 520.03 (M + 1), 1038.02 (2M + 1); Anal. Calcd for $C_{31}H_{42}N_4O_3$: C, 71.78; H, 8.16; N, 10.80. Found: C, 71.88; H, 8.35; N, 10.83.

1-(5,5-Dibenzyl-4,6-dioxo-1,4,5,6-tetrahydro-pyrimidin-2-yl)-3-isobutyl-urea 1c. Following the similar procedure for the synthesis of **1a** and using 2-amino-5,5-dibenzyl-1*H*-pyrimidine-4,6-dione (2.0 g, 6.5 mmol), **1c** was synthesized (1.9 g, 72%), which could be further easily crystallized from DCM/petroleum ether to give large crystals. mp 157−158 °C; IR ($CHCl_3$) ν (cm^{-1}): 3230, 3062, 3031, 2962, 1706, 1612, 1571, 1529, 1244; ^{1}H NMR (500 MHz, $CDCl_3$): δ 12.32 (s, 1H), 10.50 (s, 1H), 9.02 (s, 1H), 7.23−7.08 (m, 10H), 3.36 (q, 4H, $J = 13.0$, 14.5 Hz), 3.07 (t, 2H, $J = 6.1$ Hz), 1.91 (sept., 1H, $J = 6.5$ Hz),

1.00 (d, 6H, $J = 6.9$ Hz); ^{13}C NMR (125 MHz, $CDCl_3$): δ 181.9, 171.7, 157.2, 155.4, 135.1, 129.6, 128.4, 127.3, 62.1, 47.7, 45.0, 28.4, 20.1; ESI Mass: 407.05 (M + 1), 814.05 (2M + 1); Anal. Calcd for $C_{23}H_{26}N_4O_3$: C, 67.96; H, 6.45; N, 13.78. Found: C, 67.85; H, 6.57; N, 13.61.

1-(4,6-Dioxo-5,5-di-*n*-propyl-1,4,5,6-tetrahydro-pyrimidin-2-yl)-3-isobutyl-urea 1d. 1-(5,5-Diallyl-4,6-dioxo-1,4,5,6-tetrahydro-pyrimidin-2-yl)-3-isobutyl-urea **1a** (300 mg, 1.0 mmol) was subjected to hydrogenation with 10% Pd/C (60 mg) under balloon atmosphere for 12 h. Purification by recrystallization from petroleum ether afforded needle-shaped crystals of **1d** (203 mg, 67%). mp 161 °C; IR ($CHCl_3$) ν (cm^{-1}): 3232, 3062, 3026, 2964, 1706, 1614, 1571, 1529, 1463, 1245; ^{1}H NMR (500 MHz, $CDCl_3$): δ 12.71 (s, 1H), 11.51 (s, 1H), 9.17 (s, 1H), 3.11 (t, 2H, $J = 6.2$ Hz), 1.97−1.83 (m, 5H), 1.28−1.15 (m, 4H), 0.93 (d, 6H, $J = 6.6$ Hz), 0.86 (t, 6H, $J = 7.3$ Hz); ^{13}C NMR (125 MHz, $CDCl_3$): δ 183.8, 173.1, 158.0, 155.8, 58.4, 47.6, 41.8, 28.2, 20.0, 18.6, 14.0; ESI Mass: 311.05 (M + 1), 622.03 (2M + 1); Anal. Calcd for $C_{15}H_{26}N_4O_3$: C, 58.04; H, 8.44; N, 18.05. Found: C, 58.37; H, 8.16; N, 17.82.

2-[3-(5,5-Diallyl-4,6-dioxo-1,4,5,6-tetrahydro-pyrimidin-2-yl)-ureido]-benzoic Acid Isopropyl Ester 1e. Following the similar procedure for the synthesis of **1a** and using 2-amino-5,5-diallyl-1*H*-pyrimidine-4,6-dione (0.5 g, 2.4 mmol), **1e** was synthesized (0.8 g, 80%), which could be further easily crystallized from DCM/petroleum ether to give large crystals. mp 140−141 °C (DCM/petroleum ether); IR ($CHCl_3$) ν (cm^{-1}): 3265, 3083, 3020, 2981, 1730, 1689, 1652, 1585, 1512, 1442, 1377, 1255; ^{1}H NMR (500 MHz, $CDCl_3$): δ 12.06 (s, 1H), 11.09 (s, 1H), 8.18 (b, 1H), 8.56 (d, 1H, $J = 8.45$ Hz), 8.03 (d, 1H, $J = 7.65$ Hz), 7.54 (t, 1H, $J = 8.03$ Hz), 7.08 (t, 1H, $J = 7.65$ Hz), 5.70−5.63 (m, 2H), 5.28−5.14 (m, 5H), 2.75 (d, 2H, $J = 7.65$ Hz), 1.39 (d, 6H, $J = 6.12$ Hz); ^{13}C NMR (75 MHz, $CDCl_3$): δ 171.6, 169.7, 167.1, 160.3, 149.7, 141.0, 133.9, 130.7, 130.4, 122.1, 120.9, 119.4, 115.7, 68.8, 57.8, 42.1, 21.7; ESI Mass: 413.3 (M + 1), 825.6 (2M + 1); Anal. Calcd. for $C_{21}H_{24}N_4O_5$: C, 61.16; H, 5.87; N, 13.58. Found: C, 61.22; H, 5.84; N, 13.55.

Acknowledgment. P.K.B. is thankful to CSIR, New Delhi, for a Junior Research fellowship. We gratefully acknowledge the constant encouragement of Dr. S. Sivaram, Director, NCL and Dr. K. N. Ganesh, Head of the Division, NCL.

Supporting Information Available: General experimental procedures, ^{1}H and ^{13}C NMR spectra and ESI mass spectra of **1a**−**e** (PDF), and crystallographic data of **1a**−**c**,**e** (CIF). This material is available free of charge via the Internet at http://pubs.acs.org.

JO0508705